

# OPTIMIZATION OF 3D PRINTED CONTINUOUS CARBON FIBER REINFORCED PETG COMPOSITES

Anh-Duc Le\*, André Chateau Akué Aséko and Benoît Cosson

IMT Nord Europe, Institut Mines-Télécom, Univ Lille, Centre for Materials and Processes,  
F-59653 Villeneuve d'Ascq, Lille, France.

\*Corresponding author (anh-duc.le@imt-nord-europe.fr)

**Keywords:** Additive manufacturing, Continuous carbon fiber reinforced composites, Mechanical properties, Analysis of variance, Response surface methodology

## ABSTRACT

Recently, additive manufacturing (or 3D printing) of continuous carbon fiber reinforced composites (CCFRCs) based on Fused Filament Fabrication (FFF) has achieved great potential for producing complex geometries, excellent mechanical performances, and light-weight structures. However, due to the inherent design of layer-by-layer production, the 3D printed continuous carbon fiber reinforced composites (CCFRCs) remain still limited by the orientation of the fibers in the printing planes and the weakness of inter-layer strength. To ensure optimal performance in targeted applications, it is imperative to maximize the mechanical properties of the composites in question. Therefore, this study aims to optimize the printing parameters (i.e. nozzle temperature, and layer height) in order to maximize the mechanical properties of the 3D printed carbon fiber-reinforced PETG composites. An analysis of variance (ANOVA) was performed, to analyze the effect of the printing parameters on the tensile strength and the interlaminar shear strength. It was possible to conclude that both studied parameters have a dramatic impact on the targeted responses. Finally, a response surface methodology (RSM) was applied to carry out the optimal range of values for the printing parameters that satisfies the requirements for the mechanical performance of the targeted applications.

## 1 INTRODUCTION

Additive manufacturing (or 3D printing) technology has offered the creation of intricate and lightweight components at a reduced cost. Polyethylene terephthalate glycol (PETG) has emerged as a viable alternative to conventional polymers in the field of 3D printing, primarily owing to its exceptional chemical resistance, mechanical characteristics, and various other advantageous properties [1,2]. The incorporation of carbon fibers as a reinforcement in PETG-based composites results in exceptional mechanical performance, rendering them appropriate for a wide range of applications [3,4]. Nevertheless, due to the inherent design of layer-by-layer production, the additive manufacturing (AM) of CCFRCs remains still limited by the orientation of the fibers in the printing planes and the weakness of inter-layer strength [5–8]. This drawback becomes particularly problematic when dealing with three-dimensional complex mechanical loads in some industrial contexts. Under the circumstances, it is imperative to optimize the mechanical performances of the 3D printed PETG-based composites to achieve the requirements of the targeted applications.

The mechanical performances can be improved by postprocessing treatments [9,10], and optimization of the printing parameters [11,12]. For the first case, annealing is a heat treatment technique that is frequently employed as a postprocessing method to enhance both the mechanical characteristics and the surface appearance [13]. However, literature reports have shown that the later one is the first, and the most important step towards improving the mechanical properties of 3D printed parts [3]. From all the printing parameters, previous studies have suggested that the most important are the nozzle temperature, the layer height, the layer width, the infill density, and the printing speed [14]. Among these parameters, the nozzle temperature ( $T_n$ ) and the layer height ( $H$ ) were reported to have outstanding impacts on the mechanical performances [11,12]. The present work focuses on improvement of the tensile strength ( $\sigma$ ) and the interlaminar shear strength ( $ILSS$ ) of the 3D printed thermoplastic matrix,

PETG, composites reinforced with continuous carbon fiber (CCF), by optimization of printing parameters using the statistical response surface methodology (RSM). Based on the previous discussions, the nozzle temperature ( $T_n$ ) and the layer height ( $H$ ) were chosen as studied parameters. In order to generate the data set required for the statistical models, full factorial design of experiments (DOE) with 2 factors was conducted. An analysis of variance (ANOVA) was also performed, allows for analyzing the effect of the studied parameters and their interactions on the outcome mechanical properties. Based on the generated RSM models, a graphical of multi-response optimization was conducted to determine the suitable conditions by identification of an optimal region where the predicted means of response variables are in an acceptable range for the 3D printed composite parts.

## 2 MATERIALS, PROCESSING AND METHOD

The PETG filament, with a diameter of 1.75 mm, supplied by Polymaker™ was used as the feedstock in this study. The composite carbon fiber (CCF) is 0.35 mm in diameter, supplied by Anisoprint™, which composes of thousands of carbon fibers ( $v_f = 60\%$ ) pre-impregnated with a thermoset for providing good adhesion with the thermoplastic matrix. Specimens were manufactured using a Composer Desktop 3D printer A4 from Anisoprint™. The printing process is based on composite fiber co-extrusion technology. In this printing technology, both the polymer filament and the CCF are fed from two different spools to a common printing head (see Figure 1). By this way, the molten polymer wets the CCF in the nozzle prior to printing. G-code for 3D printed models were created using the Aura™ software. The nozzle temperature ( $T_n$ ) and the layer height ( $H$ ) were chosen as the two studied parameters, their respective levels are given in Table 1. Apart from the parameters in Table 1, all other processing parameters were fixed. The printing speed was set at 10 mm/s, the bed temperature was 80°C, and the layer width was 0.7 mm. The fill density was 100%, the fiber fill type was set to line with an angle of 0°.

Factor	Symbol	Level		
		-1	0	1
Nozzle temperature (°C)	$T_n$	220	240	260
Layer height (mm)	$H$	0.36	0.4	0.5

Table 1: Studied variables and their levels.

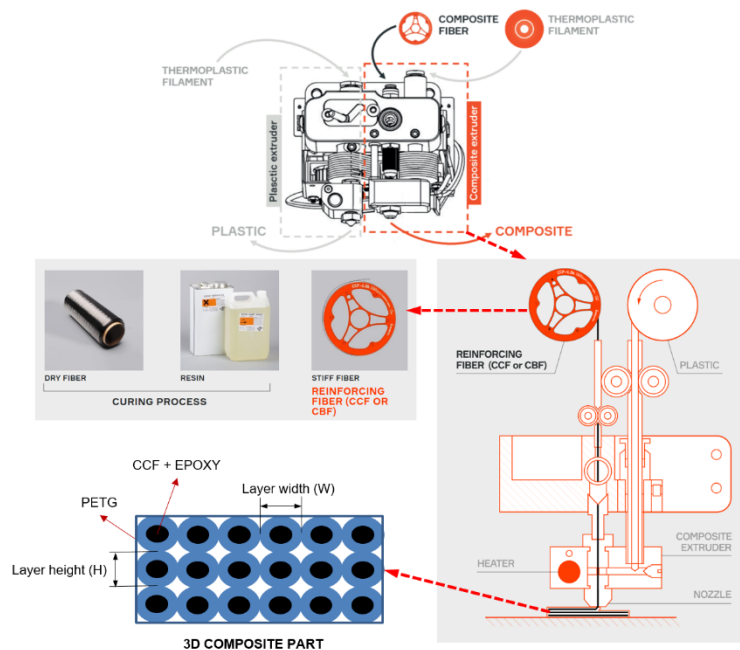


Figure 1: Schematic view of the designed Anisoprint™ printer for the CCFRCs.

The tensile strength ( $\sigma$ ) and the interlaminar shear strength (*ILSS*) of the specimens were determined according to the ISO527 and the ASTM D2344 standards respectively. Specimens of shape according to the ISO527 were prepared for tensile tests (see Figure 2). Tensile tests were performed utilizing the universal testing machine Instron 1185, with a load cell of 100 kN. The tests were performed under standardized environmental conditions, the specimens were loaded at a constant testing speed of 2mm/min until rupture. For each investigated setting, three repetitions were tested.

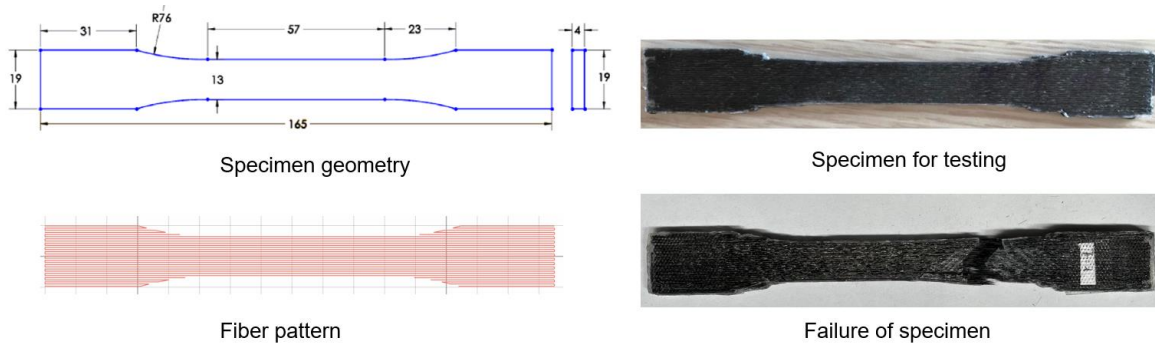


Figure 2: Preparation of specimen for tensile test and failure of specimen after tensile test.

The short beam shear (SBS) tests specimens were fabricated through two steps. First, the panels with a dimension of  $90 \times 20 \times 3 \text{ mm}^3$  were 3D printed. Then, the panels were cut into the SBS specimens with a dimension of  $18 \times 6 \times 3 \text{ mm}^3$ , according to the ASTM D2344 standard, using a saw cutter. The SBS test specimens were loaded in a 3-point bend load configuration (as shown in Figure 3) at a rate of crosshead movement of 1 mm/min. All the tests were carried out at room temperature using the universal testing machine Instron 1185, with a load cell of 10 kN. The loading nose diameter ( $D_1$ ) was 10 mm, and the support diameter ( $D_2$ ) was 3mm. The distance between the supports ( $S$ ) was adjusted to be 4-fold of the sample thickness (i.e.,  $S=12 \text{ mm}$ ). Five tests were repeated for each investigated setting to obtain the statistical distribution of the measured *ILSS*. The *ILSS* was calculated using Eq. (1) as follows:

$$ILSS = \frac{3}{4} \times \frac{P_{max}}{b \times h} \quad (1)$$

where  $P_{max}$  is the maximum load observed during and the test,  $b$  and  $h$  stand for the sample width, and the sample thickness respectively.

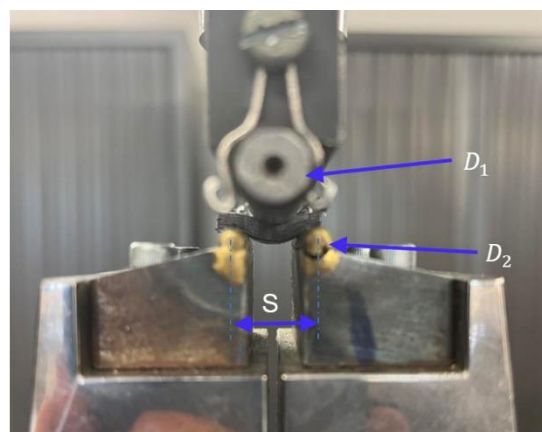


Figure 3: Short beam shear (SBS) test set-up.

Analysis of variance (ANOVA) was performed to determine the significance of the studied variables (i.e. the nozzle temperature ( $T_n$ ) and the layer height ( $H$ )) and their interactions in order of influence on

the mechanical performance of the 3D printed samples (i.e. the tensile strength ( $\sigma$ ) and the interlaminar shear strength (*ILSS*)) [15]. To generate the data set required for the statistical models, a three-level full factorial Design of experiments (DOE) with 2 factors was conducted (see Table 2). The statistical significance of the factors was defined by the probability  $p$ -value that should be lower than the alpha value set to 0.05.

The response surface method (RSM) was then applied for the prediction of the mechanical performance as a continuous function of the studied parameters [10]. RSM explores the relation between the factors ( $X_1, X_2, \dots, X_n$ ) and the response  $Y$  by fitting a quadratic polynomial to an experiment data set, as expressed in Eq. (2):

$$Y = \beta_0 + \sum_{i=1}^N \beta_i X_i + \sum_{i=1}^N \beta_{ii} X_i^2 + \sum_{i \neq j}^N \beta_{ij} X_i X_j + \varepsilon \quad (2)$$

where  $\beta_0, \beta_i, \beta_{ii}, \beta_{ij}$ , and  $\varepsilon$  are the regression coefficients for the intercept, linear, quadratic, interaction terms, and experimental error respectively. Finally, obtained response surface functions were used to determine the optimum levels of each factor to achieve the required mechanical performances.

### 3 RESULTS AND DISCUSSION

The DOEs tests and the experimental results for the tensile strength ( $\sigma$ ) and the interlaminar shear strength (*ILSS*) of the 3D printed samples at different conditions, are shown in Table 2. The highest tensile strength of 435.82 MPa was achieved at the highest nozzle temperature of 260°C, with the smallest layer height of 0.36 mm. Conversely, the smallest tensile strength of 324.84 MPa was found at the nozzle temperature and layer height of 220°C and 0.5 mm, respectively. The results of ANOVA for tensile strength is shown in Table 3. It is observed that both the nozzle temperature ( $T_n$ ) and the layer height ( $H$ ) are significant terms as their  $p$ -values are much smaller than 0.05. Especially, the tensile strength ( $\sigma$ ) is substantially dependent on the layer height (i.e.  $p$ -values <0.001). This can be explained by the fact that the effect of the layer height on the tensile strength is directly related to the changes carbon fiber content in the composite specimens. On the contrary, the tensile strength is considered to be independent on the interaction between the factors (i.e.  $p$ -values = 0.367  $\gg$  0.05).

Run	Variables		Responses	
	$T_n$ (°C)	$H$ (mm)	Tensile strength $\sigma$ (MPa)	ILSS (MPa)
1	220	0.36	412.61±4.41	22.78±1.24
2	240	0.36	413.44±12.83	24.15±0.23
3	260	0.36	435.82±4.09	26.47±0.53
4	220	0.4	381.45±18.59	22.71±0.51
5	240	0.4	391.70±4.34	23.21±0.60
6	260	0.4	408.07±8.29	24.95±0.35
7	220	0.5	324.84±6.33	20.41±0.23
8	240	0.5	330.21±7.91	20.70±1.06
9	260	0.5	377.50±20.05	21.25±0.87

Table 2: Experimental results according to DOEs

Source	DF	Adj SS	Adj MS	F-Value	$p$ -Value	Remark
$T_n$ (°C)	2	6059.4	3029.7	12.61	0.004	Significant
$H$ (mm)	2	27063.2	13531.6	56.32	<0.001	Significant
$T_n \times H$	4	1101.1	275.3	1.15	0.367	Insignificant
Error	18	4324.7	240.3			
Total	26	38548.4				

Table 3: ANOVA analysis for tensile strength

Table 4 represents the results of ANOVA for the interlaminar shear strength (*ILSS*) of the 3D printed composites. From the table, it can be seen that both studied parameters have a dramatic impact on this response (i.e. *p*-values <0.001). Also, the interaction between two factors exhibited a less significant influence on the *ILSS* due to the *p*-values of 0.05. Figure 4 shows the specimens' cross-sections and the optical micrographs of the specimens' fractures after SBS tests. It is shown that the nozzle temperature has substantial effects on microstructure and thus on interlayer bonding of the 3D printed composite parts. Higher nozzle temperatures result in lower porosity and higher interlayer bonding in the parts. In fact, the viscosity of the thermoplastic is decreasing with temperature increase, which enhances molecular mobility and flowability of the melt. Also, higher nozzle temperature carries more thermal energy, keeping thermoplastic at contact interface above its glass transition temperature longer, facilitating interdiffusion across the interface. Additionally, small layer height increases the contact pressure between nozzle and deposited material, improving the bonding quality and further promote the mechanical performance.

Source	DF	Adj SS	Adj MS	F-Value	<i>p</i> -Value	Remark
$T_n(^{\circ}\text{C})$	2	39.953	19.9767	19.81	<0.001	Significant
$H(\text{mm})$	2	111.779	55.8895	55.41	<0.001	Significant
$T_n \times H$	4	10.643	2.6607	2.64	0.05	Insignificant
Error	36	36.311	1.0086			
Total	44	198.686				

Table 4: ANOVA analysis for *ILSS*

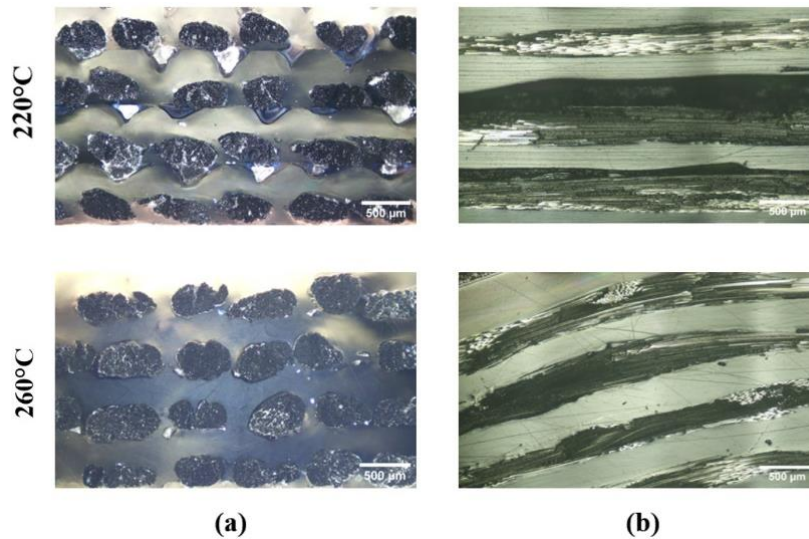


Figure 4: (a) Cross-sections of specimens (b) Optical micrographs of the specimens after SBS tests.

The generated RSM models based on the data set on Table 2, and the corresponding  $R^2$  and *p*-values can be seen in Table 5. The graph response surfaces with respect to the two studied factors are plotted in Figure 5. Both models show high values of  $R^2$  and particularly low *p*-values, which indicated that both outcome responses were predicted with a high degree of accuracy by the generated models.

Response	RSM models	$R^2$	<i>p</i> -Value
Tensile strength $\sigma(\text{MPa})$	$2855.9513 - 15.3756 \times T_n - 2.9492 \times H$ $+ 5.4983 \times T_n \times H + 0.0290 \times T_n^2$ $+ 1260.0455 \times H^2$	0.9898	0.0034
<i>ILSS</i> (MPa)	$21.0716 - 0.2298 \times T_n + 132.8476 \times H$ $- 0.4796 \times T_n \times H + 0.0010 \times T_n^2$ $- 51.2497 \times H^2$	0.9934	0.0018

Table 5: RSM models.

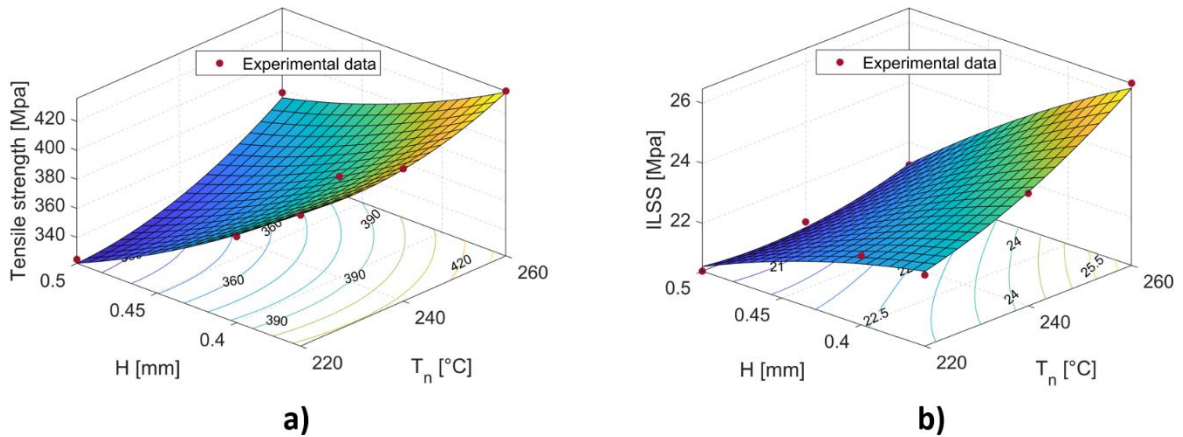


Figure 5: Response surface of tensile strength, and ILSS as a function of nozzle temperature and layer height.

Based on the proposed SRM models, a graphical of multi-response optimization was conducted to determine the best combination of printing parameters by identification of an optimal region where the predicted means of response variables are in an acceptable range for the 3D printed composite parts. In this study, the criteria applied for the determination of the optimal region were tensile strength ( $\sigma > 390 \text{ MPa}$ ) and interlaminar shear strength ( $ILSS > 23 \text{ MPa}$ ). Based on these conditions, the optimal region for printing parameters was defined as the green area in Figure 6.

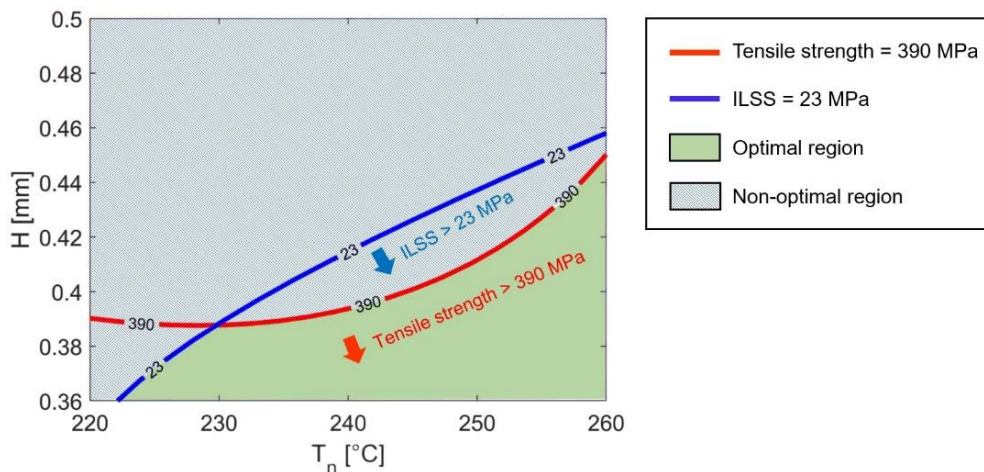


Figure 6: Design of multi-response optimization based on mechanical performance according to nozzle temperature and layer height.

#### 4 CONCLUSIONS

This study presents a procedure for optimizing the mechanical performance of 3D printed continuous carbon fiber reinforced PETG composites. The main criteria for constraint optimization were the maximum as possible the tensile strength ( $\sigma$ ) and the interlaminar shear strength ( $ILSS$ ). Envisaged parameters were the nozzle temperature, and the layer height. Analysis of variance (ANOVA) was performed which has showed the highly significant influences of both input factors on the outcome responses. Subsequently, a surface response methodology (RSM) was employed to identify an optimal region satisfying all criteria for the optimization procedure. This enabled the determination of a suitable range of values for the nozzle temperature, and the layer height that meets all the requirements for the mechanical performance of the 3D printed composites.

## ACKNOWLEDGEMENTS

This work could not be possible without the ANR JCJC SHORYUKEN which is funded by the National French Research Agency under the AAPG 2021 - CE10 «Industrie et usine du futur: Homme, organisation, technologies»

## REFERENCES

- [1] Hsueh M-H, Lai C-J, Wang S-H, Zeng Y-S, Hsieh C-H, Pan C-Y, et al. Effect of Printing Parameters on the Thermal and Mechanical Properties of 3D-Printed PLA and PETG, Using Fused Deposition Modeling. *Polymers* 2021;13:1758. <https://doi.org/10.3390/polym13111758>.
- [2] Subbarao CV, Reddy YS, Inturi V, Reddy MI. Dynamic Mechanical Analysis of 3D Printed PETG Material. *IOP Conf Ser Mater Sci Eng* 2021;1057:012031. <https://doi.org/10.1088/1757-899X/1057/1/012031>.
- [3] Valvez S, Silva AP, Reis PNB. Optimization of Printing Parameters to Maximize the Mechanical Properties of 3D-Printed PETG-Based Parts. *Polymers* 2022;14:2564. <https://doi.org/10.3390/polym14132564>.
- [4] Rijckaert S, Daelemans L, Cardon L, Boone M, Van Paepegem W, De Clerck K. Continuous Fiber-Reinforced Aramid/PETG 3D-Printed Composites with High Fiber Loading through Fused Filament Fabrication. *Polymers* 2022;14:298. <https://doi.org/10.3390/polym14020298>.
- [5] Caminero MA, Chacón JM, García-Moreno I, Reverte JM. Interlaminar bonding performance of 3D printed continuous fibre reinforced thermoplastic composites using fused deposition modelling. *Polym Test* 2018;68:415–23. <https://doi.org/10.1016/j.polymertesting.2018.04.038>.
- [6] Kabir SMF, Mathur K, Seyam A-FM. A critical review on 3D printed continuous fiber-reinforced composites: History, mechanism, materials and properties. *Compos Struct* 2020;232:111476. <https://doi.org/10.1016/j.compstruct.2019.111476>.
- [7] Wang F, Zhang Z, Ning F, Wang G, Dong C. A mechanistic model for tensile property of continuous carbon fiber reinforced plastic composites built by fused filament fabrication. *Addit Manuf* 2020;32:101102. <https://doi.org/10.1016/j.addma.2020.101102>.
- [8] Li L, Liu W, Sun L. Mechanical characterization of 3D printed continuous carbon fiber reinforced thermoplastic composites. *Compos Sci Technol* 2022;227:109618. <https://doi.org/10.1016/j.compscitech.2022.109618>.
- [9] Pazhamannil RV, Namboodiri VNJ, Hadidi HM, Edacherian A, Govindan P. Thermal post-processing effects on the polycarbonate acrylonitrile butadiene styrene composites manufactured by fused filament fabrication. *Polym Eng Sci* 2023. <https://doi.org/10.1002/pen.26274>.
- [10] El Magri A, El Mabrouk K, Vaudreuil S, Chibane H, Touhami ME. Optimization of printing parameters for improvement of mechanical and thermal performances of 3D printed poly(ether ether ketone) parts. *J Appl Polym Sci* 2020;137:49087. <https://doi.org/10.1002/app.49087>.
- [11] Spoerk M, Arbeiter F, Cajner H, Sapkota J, Holzer C. Parametric optimization of intra- and inter-layer strengths in parts produced by extrusion-based additive manufacturing of poly(lactic acid). *J Appl Polym Sci* 2017;134:45401. <https://doi.org/10.1002/app.45401>.
- [12] Garmabi MM, Shahi P, Tjong J, Sain M. 3D printing of polyphenylene sulfide for functional lightweight automotive component manufacturing through enhancing interlayer bonding. *Addit Manuf* 2022;56:102780. <https://doi.org/10.1016/j.addma.2022.102780>.
- [13] Sathish Kumar K, Soundararajan R, Shanthosh G, Saravanakumar P, Ratteesh M. Augmenting effect of infill density and annealing on mechanical properties of PETG and CFPETG composites fabricated by FDM. *Mater Today Proc* 2021;45:2186–91. <https://doi.org/10.1016/j.matpr.2020.10.078>.
- [14] Mohamed OA, Masood SH, Bhowmik JL. Optimization of fused deposition modeling process parameters: a review of current research and future prospects. *Adv Manuf* 2015;3:42–53. <https://doi.org/10.1007/s40436-014-0097-7>.
- [15] Durgashyam K, Indra Reddy M, Balakrishna A, Satyanarayana K. Experimental investigation on mechanical properties of PETG material processed by fused deposition modeling method. *Mater Today Proc* 2019;18:2052–9. <https://doi.org/10.1016/j.matpr.2019.06.082>.